

Enhanced predictive skills in physically-consistent way: Physics Informed Machine Learning for Hydrological Processes

Pravin Bhasme ¹, Jenil Vagadiya ², Udit Bhatia ¹

¹Civil Engineering Discipline, Indian Institute of Technology, Gandhinagar, India

²Computer Science and Engineering Discipline, Indian Institute of Technology, Gandhinagar, India

Key Points:

- Model to combine predictive ability of machine learning with process understanding of physics-based models for hydrological processes.
- Variants of architecture adapted for uncertainty quantification in both target (stream-flow) and intermediate variables (evapotranspiration).
- Performance gains in prediction of target and intermediate variables; annual water balance analysis reveals physical consistency of model.

Abstract

Current modeling approaches for hydrological modeling often rely on either physics-based or data-science methods, including Machine Learning (ML) algorithms. While physics-based models tend to rigid structure resulting in unrealistic parameter values in certain instances, ML algorithms establish the input-output relationship while ignoring the constraints imposed by well-known physical processes. While there is a notion that the physics model enables better process understanding and ML algorithms exhibit better predictive skills, scientific knowledge that does not add to predictive ability may be deceptive. Hence, there is a need for hybrid modelling approach to couple ML algorithms and physics-based model in synergistic manner. Here we develop a Physics Informed Machine Learning (PIML) model that combines the process understanding of conceptual hydrological model with predictive abilities of state-of-the-art ML models. We apply the proposed model to predict the monthly time series of the target (streamflow) and intermediate variables (actual evapotranspiration) in the Narmada river basin in India. Our results show the capability of the PIML model to outperform a purely conceptual model (*abcd* model) and ML algorithms while ensuring the physical consistency in outputs validated through water balance analysis. The systematic approach for combining conceptual model structure with ML algorithms could be used to improve the predictive accuracy of crucial hydrological processes important for flood risk assessment.

1 Introduction

Streamflow prediction, flood protection, and water resource management challenges continue to be highly relevant for societal as well as economic security and well-being (Butts et al., 2004; Niu & Feng, 2021). With the ever-increasing availability of computational resources, diverse spatiotemporal datasets from remotely-sensed and in-situ measurements, and advances in Machine Learning (ML) algorithms, data-driven approaches are being used widely to predict the response of catchments to meteorological forcings, including precipitation and surface temperature (Tongal & Booij, 2018; Parisouj et al., 2020; Feng et al., 2020). Despite recent advances in their predictive performance and ability to handle highly complex spatiotemporal datasets, the success of ML algorithms in the domain applications remains elusive due to limited interpretability (Gilpin et al., 2018), physical inconsistencies and persistent issues of equifinality (different model structures and parameterization schemes giving the same end state with equal accuracy) (Schmidt et al., 2020; Beven, 2006). To address interpretability challenges, physics-based models, which encapsulate our domain knowledge and physics principles, including conservation of mass, energy, and momentum through mathematical equations, remain the tool of choice for researchers and practitioners (Vieux et al., 2004; Beven, 1989). Physics-based models are broadly categorized as conceptual models and physically-based models. These models involve mathematical and semi-empirical equations with the physical basis (Devia et al., 2015). In addition to meteorological and hydrological observations, these models' predictive performance critically relies on identifying the right set of parameters, which is typically achieved through the process of calibration (Fenicia et al., 2007). While there is a notion that physics-based models enable better process understanding, and ML methods lead to better predictive skills, the process understanding that does not add to predictive ability may be specious, and improved predictive skills devoid of physical realism may not generalize to unexpected, yet possible scenarios (Ganguly et al., 2014). With the growing realization that neither purely ML algorithms nor physics-based models suffice to address the domain-specific challenges, physics guided machine learning approaches are gaining significant attention in scientific and engineering domains, aiming to integrate the data and scientific knowledge in a complementary manner (Muralidhar et al., 2019; Wang et al., 2017; Zhang et al., 2020).

Multiple frameworks, both conceptual and applied, for combining physics with machine learning approaches have been proposed in the literature for diverse applications.

For example, Wagner and Rondinelli (2016) have demonstrated the importance of scientific reasoning for discovering reliable structure, property, and processing models, as well as listed nuances associated with machine learning applications in material science. Wang et al. (2017) have proposed a data-driven, physics-informed machine learning (PIML) approach for reconstructing discrepancies in Reynolds-averaged Navier Stokes modeled Reynolds stresses. It is achieved by training existing direct numerical simulation databases through machine learning techniques and applied the PIML approach for different flow conditions such as turbulent flows developed in the square duct for varying Reynolds numbers and flows with massive separation. Muralidhar et al. (2019) have demonstrated the application of physics-guided model architecture for predicting drag force acting on each particle in fluid flow. Further, they have incorporated physics-based loss functions to capture physical knowledge, avoid constraint violation, and develop a physics-guided deep neural network model. For seismic response modeling, Zhang et al. (2020) have developed a physics-guided convolutional network architecture to predict a building’s seismic response. Faghmous et al. (2014), Reichstein et al. (2019), and Ganguly et al. (2014) have highlighted the need to have scalable data science methods which can incorporate physical and conceptual understanding for better interpretation for applications in earth and atmospheric sciences. The authors themselves noted that while there exist multiple opportunities in the area of incorporating contextual cues from the domain into machine learning models, the domain-specific challenges (that is, preservation of spatiotemporal structures, confidence and uncertainty representation in predictions) should be accounted for to ensure physical consistency in the outputs.

Karpatne et al. (2017) and Jia et al. (2019) developed physics-guided variants of ML models that guide neural network architectures to simulate lake temperature profiles in a physically consistent manner. Specifically, Karpatne et al. (2017) demonstrated how to combine the standard neural network models with the energy conservation laws to outperform purely knowledge-based or data-driven models. These goals were achieved in two ways. First, the outputs from physics-based models were fed into ML architecture. Secondly, they introduced physical knowledge-based constraints in the temporal ML model’s objective function (Long Short Term Memory (LSTM) in this case). Liang et al. (2019) generated a database through simulations of the physics-based model and then processed it with different data-driven approaches to predict the quantity and quality of surface water in agricultural fields. Recently, Lu et al. (2021) introduced a physics-informed LSTM model to improve the prediction when data is out of distribution. The physics-based Precipitation Runoff Modeling System (PRMS) model-simulated streamflow and meteorological features were given as inputs to the LSTM for the streamflow prediction. We argue that while these approaches could help to improve the predictive abilities of purely physics-driven or ML models, the gains in terms of interpretability and capability of these hybrid models to capture the intermediate variables realistically are yet to be explored. Khandelwal et al. (2020) has proposed the LSTM based architecture for streamflow prediction, which emulates the Soil and Water Assessment Tool (SWAT), a physically-based semi-distributed model. They used the same inputs as the SWAT model into three LSTMs in the first layer to simulate soil water, evapotranspiration, and snowpack. The outputs obtained from the first layer were combined with the original SWAT inputs to feed into another LSTM to model the streamflow. We note that this is one of a few physics-guided data sciences approaches for hydrological modeling that accounts for intermediate variables (i.e., soil water, evapotranspiration, and snowpack). However, a typical SWAT architecture involves multiple intermediate fluxes (e.g., evapotranspiration, surface runoff, groundwater flow, percolation, lateral flow, groundwater recharge, deep aquifer recharge) and state variables (e.g., soil water, snowpack, deep aquifer storage, shallow aquifer storage) (Neitsch et al., 2004), which were altogether ignored in their architecture, hence limiting the interpretability of outputs.

In this study, we design a modeling framework to combine the conceptual hydrological model with state-of-the-art ML models to leverage ML algorithms’ predictive abil-

ity with process understanding of physics-based models in a synergistic manner. Specifically, we use the structure of the *abcd* model to identify the input (precipitation, potential evapotranspiration, groundwater storage, and soil moisture), intermediate (actual evapotranspiration), and target variables (streamflow at particular gauge location) at various steps (Figure 1c). Then, we replace empirical equations of our conceptual model (the *abcd* model) with ML algorithms at various steps to identify the relationships between input and output (both intermediate and target) variables. Our model design is inspired by the fact that conceptual hydrological models involve empirical and semi-empirical equations, which are generally developed and validated for specific basins. Therefore, their application outside the basin boundaries calls for abundant caution. We argue that the use of ML algorithms to identify the complex relationships between input and output variables at various stages of the modeling process adds flexibility to the models having rigid mathematical structures. Hence, PIML models can generalize to the basins where empirical equations of conceptual models may not generalize. We demonstrate the PIML models’ ability to capture the intermediate variables with greater accuracy, which in turn transpire into better model performance to model target variable (streamflow in the present case) compared to conceptual and pure data-driven architectures. Finally, we demonstrate the ability of variants of the PIML models to capture the water balance effectively. We demonstrate the proposed model’s applicability on the Narmada River Basin with gauge station at Sandia (Figure 1d). We use a suite of Machine Learning and Deep Learning architectures commonly used in numerous hydrological and earth sciences applications, including LSTMs (Kratzert et al., 2018), Least absolute shrinkage and selection operator (LASSO) and Ridge Regression (Yu & Liong, 2007; Lange & Sippel, 2020), Support Vector Regression (Deka et al., 2014), Gaussian Process Regression (Sun et al., 2014), and Bayesian LSTMs (Lu et al., 2021) for purely ML-based as well as hybrid PIML models.

We organize the rest of the manuscript as follows: in section 2, we present the brief overview of the conceptual *abcd* model and ML algorithms used in this study. Details of the proposed PIML model and various evaluation metrics deployed in this study are also discussed. In section 3, we discuss the details of the study area and datasets used in this research. In section 4, we compare physics-based, ML, and PIDS algorithms using metrics discussed in section 2. Finally, we discuss the physical consistency of PIML models by performing a water-balance analysis.

2 Methods

This section presents the review of the conceptual *abcd* model and various ML models with underlying equations used in this study. Further, we discuss the architecture of the PIML model. Finally, we present a brief overview of various performance metrics used throughout this study.

2.1 Review of the *abcd* model

The *abcd* model is a simple Water Balance (WB) conceptual hydrological model proposed by Thomas (1981). While it was originally developed to examine the catchment scale water balances at annual scales, variants of the model have been applied for regional and local hydrological investigations at monthly scales (Alley, 1984; Vandewiele et al., 1992). The conceptual model involves the parsimonious yet adequate description of various hydrological processes at catchment scale with the lesser computational cost making it highly popular in operational and research practice (Clark & Kavetski, 2010). Specifically, the *abcd* model structure has been widely used for hypotheses testing, model performance evaluation (Martinez & Gupta, 2010; Bai et al., 2015), and hydrological uncertainty reduction experiments (W. Li & Sankarasubramanian, 2012) owing to a highly realistic representation of various hydrological processes despite its simple structure. Fig-

Figure 1a shows the conceptual representation of the *abcd* model. The model consists of two storage compartments: soil moisture storage and groundwater storage. Inputs required are monthly precipitation (P_t) and potential evapotranspiration (PET_t), while output generated is streamflow (Q_t). This model is calibrated with four parameters, a , b , c , and d . The parameter a , ($0 < a \leq 1$) controls the amount of direct runoff when soil is unsaturated, and parameter b reflects the upper bound of the total of actual evapotranspiration (ET_t) and soil moisture (SM_t) at a given time step. The groundwater recharge (GR_t) is controlled by parameter c , while parameter d , decides the amount of groundwater storage (GW_t) to be converted to groundwater discharge (GD_t). The direct runoff and groundwater discharge together generate the streamflow. The model includes two state variables: W_t (available water) and Y_t . While W_t is the sum of precipitation (P_t) at a given time step and soil moisture (SM_{t-1}) at the previous time step, Y_t represents the sum of actual evapotranspiration (ET_t) and soil moisture (SM_t) at a given time step. Equations 1a-1b show the mass balance for soil moisture and groundwater storage compartments. Equations 1d-1e are typical examples of parameterized relationships among various variables (See Supplementary Information (SI) for complete set of equations).

$$SM_t + ET_t + DR_t + GR_t = SM_{t-1} + P_t \quad (1a)$$

$$GW_t + GD_t = GW_{t-1} + GR_t \quad (1b)$$

$$W_t = SM_{t-1} + P_t \quad (1c)$$

$$Y_t = SM_t + ET_t = \frac{W_t + b}{2a} - \sqrt{\left(\frac{W_t + b}{2a}\right)^2 - \frac{b \cdot W_t}{a}} \quad (1d)$$

$$ET_t = Y_t \times (1 - e^{-PET_t/b}) \quad (1e)$$

2.2 Review of Machine Learning Algorithms

Recent advances in the field of machine learning have provided many methodological opportunities to meet the evolving needs and challenges of hydrological research. ML models have demonstrated superior performance in learning patterns and generalizations as well as extracting patterns from complex streams of geospatial and hydrological datasets (Lange & Sippel, 2020; Reichstein et al., 2019). ML algorithms form the core of the proposed PIML model. Hence, a review of various methods used in this study is presented to clarify the subsequent sections.

Long Short Term Memory (LSTM) is an artificial neural network architecture that has gained popularity for sequential data problems. In the context of hydrology, LSTMs have been used for rainfall-runoff modeling at hourly (Xiang et al., 2020), daily (Fu et al., 2020; Cheng et al., 2020), monthly (Cheng et al., 2020) time steps as well as for the improvement in the predictions of the physics-based models (T. Yang et al., 2019). LSTMs are a special kind of recurrent neural networks (RNNs) capable of learning long-term temporal dependencies. The simple RNNs have an issue of vanishing gradient, which can be removed by LSTMs with the introduction of gates and memory cells (Hochreiter & Schmidhuber, 1997).

Bayesian Neural Networks (BNNs) have advantages over neural networks, such as they can handle small data well while generating uncertainty bounds of predictions. Since BNNs incorporate posterior inference in standard neural networks, these architectures have gained popularity for uncertainty quantification (Marshall et al., 2004; J. Yang et al., 2007; Raje & Krishnan, 2012). Recently Lu et al. (2021) has applied Bayesian LSTM for uncertainty quantification in streamflow prediction. BNNs were made by approximating the intractable Bayesian Inference. BayesByBackprop (Blundell et al., 2015) is a backpropagation-compatible algorithm to learn probability distribution of a neural network. The same concept is extended to create Bayesian LSTM. BNNs can provide us

uncertainty on weights by sampling them from a distribution parameterized by trainable variables (Esposito, 2020).

Gaussian Process Regression (GPR) is a non-parametric kernel-based probabilistic model, which has gained wider popularity in the domain of ML (Williams & Rasmussen, 2006). Unlike various ML algorithms that determine the exact values of parameters, GPR infers the probability distribution over all possible values using the prior distribution and updated distribution (known as a posterior distribution) that incorporates information from both prior distribution and available data. Researchers have used the GPR for daily (Rasouli et al., 2012) and monthly (Sun et al., 2014) streamflow forecasting.

Support Vector Machine (SVM) is developed for classification, and it is extended to regression by Vapnik (1995). Support Vector Regression (SVR) is one the most popular ML approaches used for daily (Dibike et al., 2001; Malik et al., 2020) and monthly (Maity et al., 2010) streamflow predictions. SVRs can efficiently learn the non-linear relationships between predictors (input variables) and predictands (output variables) using the kernel trick, which maps the inputs into linearly solvable high-dimensional feature spaces.

The least absolute shrinkage and selection operator (LASSO) (Tibshirani, 1996), and Ridge Regression (Hoerl & Kennard, 1970) are some of the simplest techniques which are widely used to reduce model complexity and prevent overfitting. LASSO regression works by reducing the model complexity and feature selection by penalizing the absolute sum of coefficients. As a result of this regularization, some of the coefficients that do not affect the output are reduced to zero. In Ridge regression, the square of the coefficients' magnitude is penalized instead of the absolute sum. When coefficients take large values, the objective function (typically Mean Square Error function) is penalized, resulting in the coefficients' shrinking during the optimization process. LASSO and Ridge regressions have been widely applied for streamflow forecasting, and their outputs have been found comparable with state-of-the-art ML algorithms (Lima & Lall, 2010; Chokmani et al., 2008; Xiang et al., 2020).

The details of all the ML models used in this study are presented in SI.

2.3 Physics Informed Machine Learning model

The proposed PIML model provides a way to combine the physics-based conceptual model with various ML approaches to enable better process understanding and improve predictive performance while being mindful of physical consistencies (e.g., water balance). The proposed model's premise is as follows: use the covariate structure of the physics-based conceptual model (the *abcd* model in this case) and replace rigid mathematical relationships among input and output variables at various steps using ML algorithms. While the conceptual model structure provides the physics-informed choice of covariates and interpretable structure, ML algorithms help in extracting complex relationships between the input and output variables. For example, in the *abcd* model, ET_t is non-linear function of SM_{t-1} , PET_t , and P_t (Equations 1c, 1d and 1e). In the PIML model, we use SM_{t-1} , PET_t , and P_t as inputs (or predictors) into our embedded ML model and obtain the estimate of ET_t using various ML algorithms (deployed independently) described in Figure 1c. The estimates of ET_t thus obtained is combined with SM_t , SM_{t-1} , GW_t , GW_{t-1} and P_t to obtain new covariate matrix, which is then fed into next layer of ML algorithm to obtain the final estimates of Q_t (target variable in this case). We note that choice of these covariates is governed by the water-balance equation (Equation 2a):

In general form, the functional relationship for the ET_t and Q_t can be written as follows.

$$Q_t = f(P_t, ET_t, SM_t, SM_{t-1}, GW_t, GW_{t-1}) \quad (2a)$$

$$ET_t = g(P_t, SM_{t-1}, PET_t) \quad (2b)$$

The exact function form of f and g is determined by embedded ML models (Figure 1c).

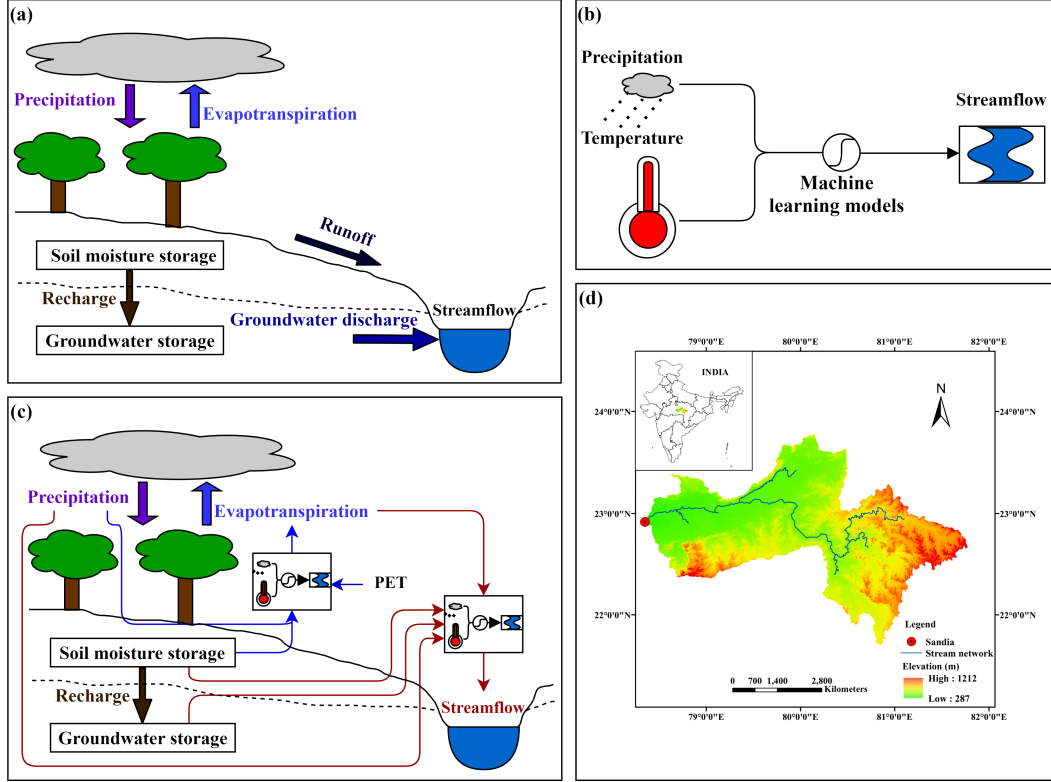


Figure 1. Illustration of different model architectures used in this study. (a) Conceptual representation of the *abcd* model. Thick arrows represent the different processes (and directions) of various fluxes in the conceptual model, whereas the rectangular boxes indicate two storage compartments (Soil moisture and groundwater) inside the model. (b) Pictorial representation of ML architecture with precipitation and temperature as input variables (predictors) and streamflow as target variable (predictand). Both linear and non-linear ML algorithms are used here. (c) Proposed PIML model architecture: the ML approach is embedded into the *abcd* model architecture. The blue arrows show functional dependencies of actual evapotranspiration (ET) on precipitation (P), soil moisture storage (SM), and potential evapotranspiration (PET). Similarly, red arrows show that evapotranspiration, groundwater, and soil moisture storages would be required predictors for streamflow estimation. (d) The details of the study area. It shows the Sandia gauge station location and digital elevation model of the part of the Narmada river basin considered in this study.

2.4 Evaluation metrics

For model performance evaluation, we have used Nash-Sutcliffe Efficiency (NSE), Percent Bias (PBIAS), Root Mean Square Error (RMSE). Widely used in various hydrological applications (Najafi & Moradkhani, 2016; Swain & Patra, 2017; Paul et al., 2019; Wagena et al., 2020), these metrics assess model efficiency, biases in the model predictions, and estimate errors in the model outputs, respectively.

2.4.1 Nash-Sutcliffe Efficiency

The NSE (Nash & Sutcliffe, 1970) is a reliable and widely used statistic to assess goodness of fit for hydrological models (McCuen et al., 2006). The NSE value has a range of $-\infty$ to 1.0. When the NSE value is 1, it shows a perfect match between modeled output and observed data, while if it is less than 0, it shows observed mean is a better predictor than the model output. Following equation shows the formula for NSE calculation:

$$NSE = 1 - \frac{\sum_{i=1}^n (O_i - S_i)^2}{\sum_{i=1}^n (O_i - \bar{O})^2} \quad (3a)$$

where, S_i , O_i , and \bar{O} are model output, observed data, and mean of observed data, respectively.

2.4.2 Percent Bias

It helps to determine how well the model can estimate the average magnitudes of the required output. The PBIAS ranges from $-\infty$ to ∞ . Its optimal value is 0, while the positive and negative values show model underpredicts and overpredicts, respectively.

$$PBIAS = \frac{\sum_{i=1}^n (O_i - S_i)}{\sum_{i=1}^n O_i} \times 100 \quad (3b)$$

2.4.3 Root Mean Square Error

It is the measure of deviations in model output from observed data. The RMSE ranges from 0 to ∞ , and when it is equal to 0, it shows both modeled output and observed data are perfectly match each other.

$$RMSE = \sqrt{\frac{\sum_{i=1}^n (O_i - S_i)^2}{n}} \quad (3c)$$

The model performance is evaluated using the criteria outlined in Moriasi et al. (2015). For monthly simulation, $NSE > 0.8$, $0.7 < NSE \leq 0.8$, $0.5 < NSE \leq 0.7$ and, $NSE \leq 0.5$, the model performance is considered as very good, good, satisfactory and unsatisfactory, respectively. Negative NSE values indicates the model performance is unacceptable.

3 Study area and datasets

To illustrate the proposed model's applicability, we have selected the part of the Narmada river basin up to gauge station located at Sandia (Figure 1d). Flowing through the states of Gujarat and Madhya Pradesh, the Narmada River is a 1312 km long river draining a 98796 km^2 area. The study area considered here has a drainage area of 38,571 km^2 . The daily precipitation and (minimum and maximum) temperature at $0.25^\circ \times 0.25^\circ$ and $1^\circ \times 1^\circ$ spatial resolution, respectively, are obtained from the India Meteorological Department (IMD) for the period of 1979 – 2014. The observed streamflow data of the Sandia gauge station (22.92°N, 78.35°E) is obtained from the India Water Resources Information System (India-WRIS; <https://indiawris.gov.in/>). The daily soil moisture, groundwater storage, and evapotranspiration are obtained from Global Land Data Assimilation System (GLDAS) Catchment Land Surface Model L4 daily datasets, available through the archives of the Goddard Earth Sciences Data and Information Services Center (GES DISC) of National Aeronautics and Space Administration (NASA) (<https://disc.gsfc.nasa.gov/>).

We calculate the potential evapotranspiration using the Hargreaves method (equation 4) (Hargreaves & Samani, 1985). The daily PET values are summed up to monthly

Table 1. Datasets used in this study

Data	Spatial resolution	Source
Precipitation	0.25°	IMD (Pai et al., 2014)
Minimum and maximum temperature	1°	IMD (Srivastava et al., 2009)
Soil moisture, groundwater storage and actual evapotranspiration	0.25°	GLDAS (B. Li et al., 2019)
Streamflow	Gauge at Sandia	India-WRIS

values, followed by spatial averaging over the study region.

$$PET = 0.0023 \times Ra \times \sqrt{(T_{max} - T_{min})} \times (T_{avg} + 17.8) \quad (4)$$

where, PET is potential evapotranspiration in mm/day and Ra is the extra-terrestrial radiation in $MJm^{-2}day^{-1}$. T_{max} , T_{min} and, T_{avg} are maximum, minimum and average surface temperature in degree Celsius respectively.

To assess the algorithm’s generalizability, we consider distinct training and testing periods while ensuring that the test set does not contain examples from the training sets. Specifically, we use the window of 1979-2008 for training and 2009-2014 for validating the models on testing data. We kept similar training and testing data for the *abcd* model, ML models, and the PIML model. The additional warm-up period required for the *abcd* model is selected as 1976-1978. Subsequently, all evaluation metrics (See Results) are calculated on the test set.

4 Results

4.1 Evaluating performance of the physics-based model

Here, we evaluate the performance of the *abcd* model in predicting target and intermediate variables. We have considered the three cases. In each case, we use the same model structure but calibrate: (a) modeled streamflow (Q) against observed Q; (b) modeled Q and ET against observed Q and ET, respectively; and (c) modeled Q, SM, GW, and ET against observed Q, SM, GW, and ET, respectively. For all these cases, we use particle swarm optimization to estimate the parameters. The model warm-up and calibration period are selected as 1976-1978 and 1979-2008, respectively. We test the calibrated model’s performance for all cases using monthly data from 2009-2014 (same as the period of testing data used in all ML algorithms throughout the study). Results for all three cases are shown in Figure 2. Table 2 summarizes the calibrated *abcd* model’s performance in terms of key performance metrics for the three cases. The model performance is evaluated using the criteria outlined in Moriasi et al. (2015). For cases (a) and (b), model performance is categorized as “very good.” In contrast, for case(c), the performance is classified as unacceptable in modeling the streamflow (based on the values of NSE). However, in case (b), despite calibrating the model for both Q and ET, the predictive performance on intermediate variable (ET) remains “unacceptable.” Further, for case (c), we observe that the model performance was “unacceptable” for all the predicted variables, including streamflow. Our results imply that while it is possible to obtain remarkable performances on target variables through the calibration process, even simple conceptual models may not simulate various intermediate processes consistently, which are otherwise important for interpretability (as observed in case (a)). The results

thus obtained underscore the need to seriously consider model structure, generalizability, and intermediate process representations in physics-based models (Kirchner, 2006).

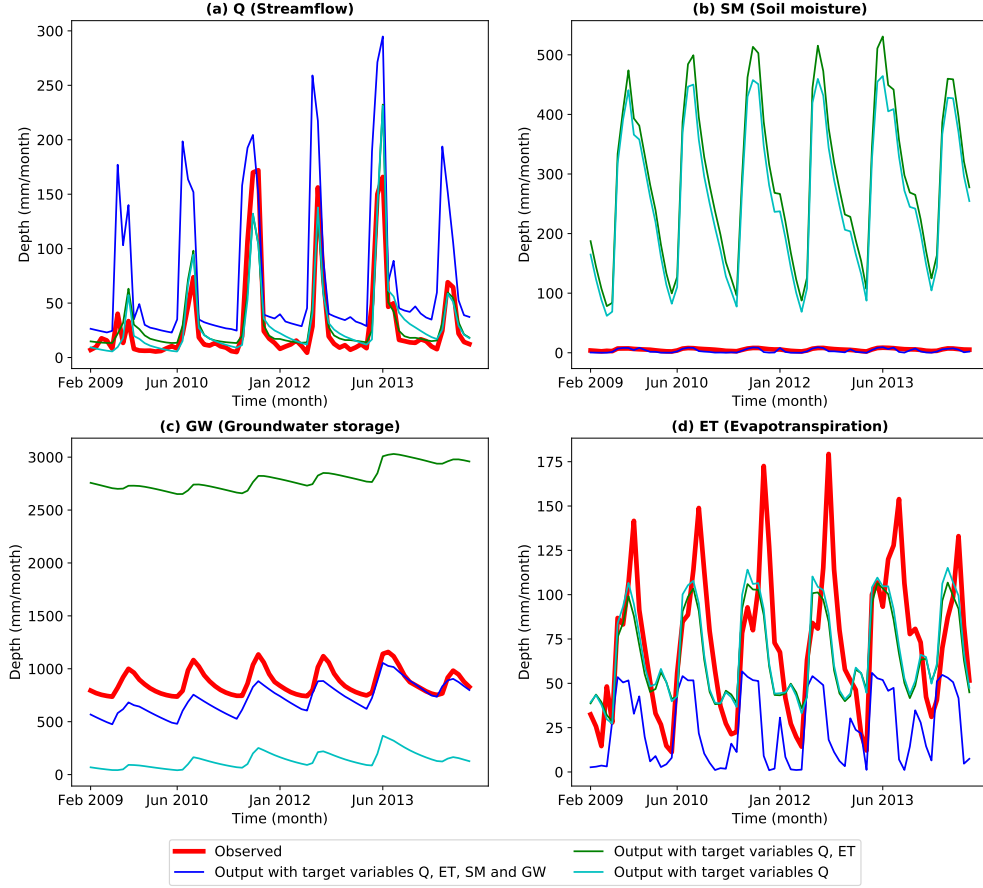


Figure 2. Time-series plots for observed data and model outputs of respective variable: (a) Q (streamflow); Streamflow prediction with model calibrated against Q and ET exhibits a good agreement with observed streamflow. When the model is calibrated against all the four variables (Q, ET, SM, GW), a dip in the performance is noted; (b) SM (soil moisture); When model calibrated against four variables Q, ET, SM, GW, the modeled SM is comparable to observed SM. For other two cases, model cases, calibrated model fails to capture the trend as well as magnitude; (c) GW (groundwater storage); For all cases, significant offset between observed and predicted values of GW time-series is noted (d) ET (evapotranspiration); same as (a) but for Actual ET.

4.2 Performance evaluation of ML Algorithms

Before we discuss the results of the PIML model, we present the performance of various ML algorithms to model streamflow with a different set of input variables. These ML algorithms would be embedded into the structure of the conceptual model. Thus, it is imperative to understand the ability of ML models to capture relatively straightforward rainfall-runoff relationships. Specifically, we use (a) inputs as precipitation and average temperature and (b) inputs as precipitation and actual evapotranspiration. Fig-

Table 2. Performance assessment during validation period (2009-2014) for ET, Q, SM and GW in the *abcd* model with model calibration against different variables

Variable	ET			Q		
Performance metric	RMSE	PBIAS	NSE	RMSE	PBIAS	NSE
(a) Target: Q	30.443	-6.495	0.438	17.767	8.392	0.815
(b) Target: Q and ET	31.519	-10.381	0.397	17.172	11.296	0.827
(c) Target: Q, ET, SM and GW	60.860	-65.289	-1.247	64.303	145.771	-1.423

Variable	SM			GW		
Performance metric	RMSE	PBIAS	NSE	RMSE	PBIAS	NSE
(a) Target: Q	286.336	4862.764	-23967.799	739.475	-84.398	-37.014
(b) Target: Q and ET	314.685	5384.296	-28948.883	1934.970	221.640	-259.286
(c) Target: Q, ET, SM and GW	2.776	-35.066	-1.253	180.558	-17.592	-1.266

Table 3. Performance assessment of ML models during the testing period (2009-2014)

Input variables	(a) P and T			(b) P and ET		
Performance metric	RMSE	PBIAS	NSE	RMSE	PBIAS	NSE
LSTM	28.104	-6.721	0.537	27.252	4.322	0.565
LASSO	28.037	-2.624	0.539	27.899	-0.312	0.544
Ridge	28.041	-2.638	0.539	27.902	-0.307	0.544
SVR	33.420	-31.625	0.346	27.098	-1.003	0.570
GPR	30.008	-2.056	0.472	27.600	1.107	0.554
Bayesian LSTM	28.198	5.684	0.534	27.730	-15.230	0.549

ure 3a and 3b shows the comparison of all the ML models with observed streamflow for both cases. Performance metrics for all the algorithms are summarized in Table 3.

For case (a), LSTM, LASSO, Ridge, Bayesian LSTM exhibit satisfactory performance, whereas performance SVR and GPR lie in the "unsatisfactory" range. Similarly, for case (b), we note that all the models' performance is in the "satisfactory" range based on the NSE criteria. Though Bayesian LSTM shows higher PBIAS, the improved NSE and decreased RMSE highlight the improvements in the model prediction, which can be attributed to input variables' choice. Further, we adapt the architecture of Bayesian LSTMs to quantify the associated epistemic uncertainty (Fig. 4). We note that despite various ML models' ability to capture the non-linear relationship between predictors and predictands and their scalability, it is often difficult for users to comprehend why specific predictions are made. Thus, there is an opportunity to combine ML and Physics-Based models' architectures in a complementary way to address the associated limitations. In this study, we achieve this by using the *abcd* model structure and embed ML algorithms in the proposed PIML model to simulate intermediate processes.

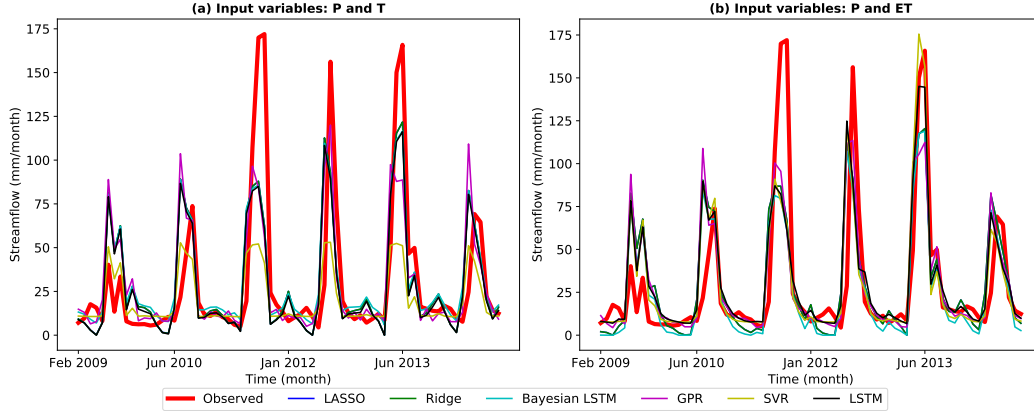


Figure 3. Time series plots of observed streamflow and modeled output of different ML models with different input variables (a) precipitation (P), average temperature (T) and, (b) precipitation (P), evapotranspiration (ET).

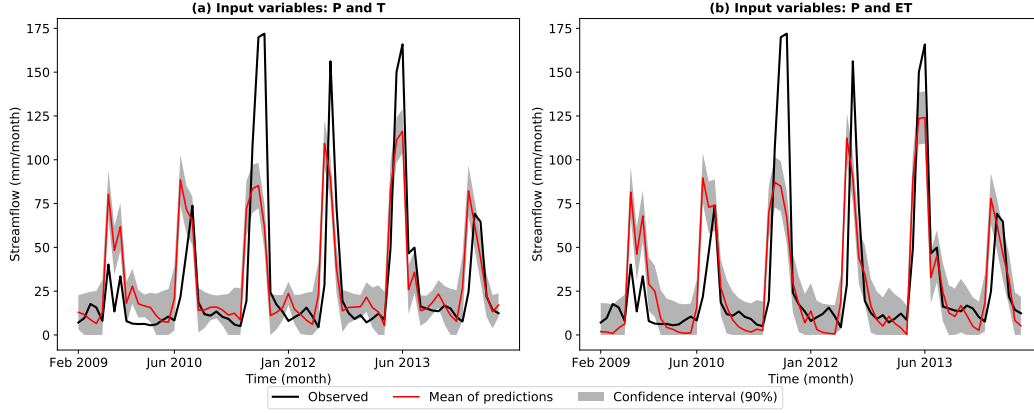


Figure 4. Time series plots of observed streamflow and modeled output of Bayesian-LSTM model at 90 percent confidence interval with different input variables (a) precipitation (P), average temperature (T) and, (b) precipitation (P), evapotranspiration (ET). The plot shows there is no reduction in uncertainty on comparing case (a) to case (b) even after changing the predictor variables.

4.3 Performance Evaluation of PIML model

We evaluate the performance of the PIML model for an intermediate variable (Actual ET) and streamflow (Q) for which credible observations are available for both training and testing periods (Figure 5a and 5b). Table 4 summarizes the results of the PIML models embedded with various ML algorithms. The NSE value for Q shows that PIML models embedded with LSTM and GPR perform "very good" while other models exhibit "good" performance. We compare the performance of the PIML approach with the corresponding ML approach. For example, the performance of the *abcd* model embedded with GPR and purely ML-based GPR algorithm are compared. We note consistent improvement in the NSE values obtained from monthly Q for all 6 cases of PIML (Table 4) compared to ML algorithms' performance (Table 3). Further, we note that the best performing PIML architectures (*abcd*+GPR, and *abcd*+LSTM) even outperform the *abcd*

Table 4. Performance assessment of PIML models during the testing period (2009-2014)

Variable	ET			Q		
Performance metric	RMSE	PBIAS	NSE	RMSE	PBIAS	NSE
LSTM	22.704	-23.966	0.687	16.083	4.124	0.848
LASSO	25.975	-3.303	0.591	20.901	3.796	0.744
Ridge	27.023	-4.013	0.557	21.02	4.259	0.741
SVR	11.703	-2.543	0.917	19.719	-4.975	0.772
GPR	16.407	-9.287	0.837	15.001	-0.626	0.868
Bayesian LSTM	41.819	41.635	-0.061	21.242	2.572	0.736

model (Table 2). Further, we calculate the model performance on predicting ET and note that 2 (PIML+SVR), (PIML+GPR) out of 6 variants of PIML exhibit "very good" performance, whereas three variants (PIML+LASSO, PIML+Ridge, PIML+LSTM) can be classified as satisfactory. These five models also outperform the *abcd* model in predicting monthly ET, thus highlighting the superiority of PIML models in predicting target and intermediate variables.

Further, we demonstrate how PIML approaches can be tailored to quantify uncertainties in the predictions of intermediate and target variables. Specifically, we quantify the uncertainties in modeled ET and Q using *abcd*+ Bayesian LSTM variant of PIML. Predictions of Q and ET with 90 percent confidence interval are shown in Figure 6a and Figure 6b, respectively, for the testing period. In addition to the superior performance of the PIML model, we also notice the reduction in uncertainty bounds in predictions of Q compared to purely ML-based algorithms (Figure 4b).

As noted earlier, in addition to improved prediction accuracy over pure physics or ML-based approaches, PIML approaches should generate outputs consistent with physical laws such as conservation of mass. In the context of hydrology, it is imperative to assess the model's ability to simulate annual water balance realistically.

To check annual water balance, the sum of precipitation should be equal to actual ET, streamflow, and change in soil moisture and groundwater storage. For our study area, soil moisture and groundwater storage changes are observed as -0.045 mm and -0.155 mm, respectively. As these values are negligible in comparison to other terms in the water balance equation, the changes in storage are thus ignored (Szilagyi, 2020).

Here, we consider three variants of PIML: (a) PIML with SVR; (b) PIML with GPR; and (c) PIML with SVR and GPR. While PIML with GPR performs the best in predicting Q, PIML with SVR outperformed other variants in predicting ET. Hence, we experiment with the hybrid variant: SVR for modeling ET in the first layer and GPR to model Q in the second layer in our PIML architecture. It is noteworthy that P, ET, and Q are obtained from three sources (Table 1). Therefore, an initial difference of -9.884 mm is observed between P and the sum of ET and Q. We calculate the percentage deviation in ET+Q for all the variants, with observations taken as a benchmark. Variant (c) exhibits deviation of -1.893 %, whereas variants (a) and (b) have the deviation of -3.255% , -6.754% respectively in annual water balance (Table 5). The lower values of % deviation for three cases demonstrate the ability of PIML approaches to simulate annual water balance consistently.

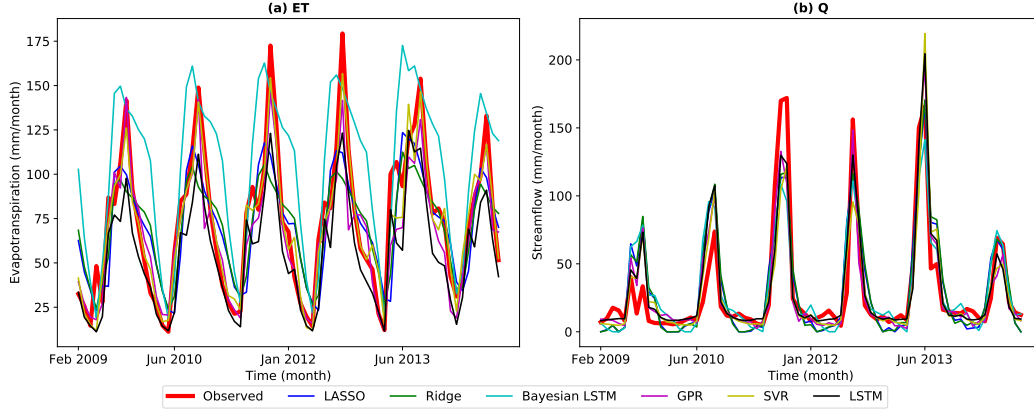


Figure 5. Time-series plots of PIML model output for (a) ET and (b) Q. Most PIML variants are able to capture trends and magnitude with reasonable performance for both the variables. For ET, we note the superior predictive performance of PIML model embedded with SVR. However, notable lag is observed in predictions obtained from PIML+Bayesian LSTM when compared to observations. For Q, all variants are consistent in their predictive performance. PIML with GPR and LSTM outperform other variants.

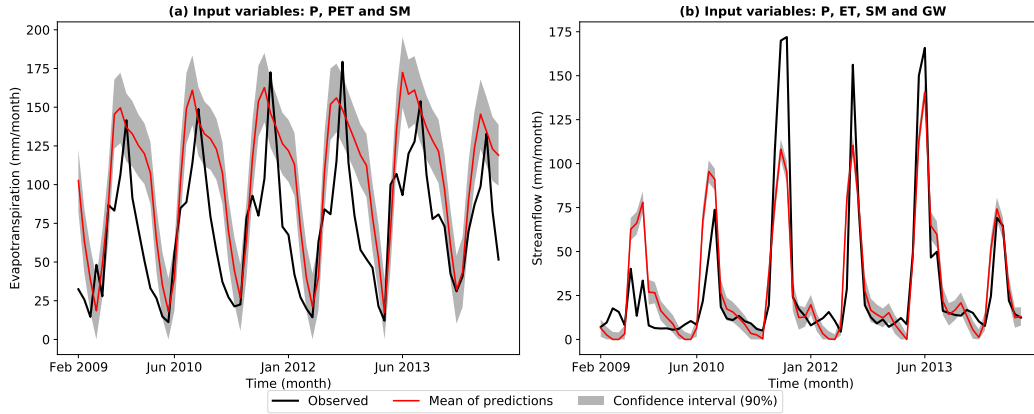


Figure 6. 90 % confidence interval bounds in the prediction of (a) ET and (b) Q as obtained from PIML model embedded with Bayesian LSTMs. For Q, considerable reduction in uncertainty bounds is reported in comparison to pure ML algorithms

5 Conclusion

Physics-guided and physics-informed data science approaches have received significant attention in the recent past (Muralidhar et al., 2019; Wang et al., 2017; Zhang et al., 2020; Karpatne et al., 2017). Several architectures in disparate fields have been proposed to improve the predictive abilities of pure physics-based and ML approaches in a physically consistent manner. Hydrological modeling is a non-linear and complex problem with ample scope for improvement. In this study, we propose the PIML model for predicting target as well as intermediate variables. We demonstrate the applicability of this model on a single hydrological unit to predict monthly time-series of actual evapotranspiration and streamflow, the two key variables in hydrological processes (Xiong et al., 2019).

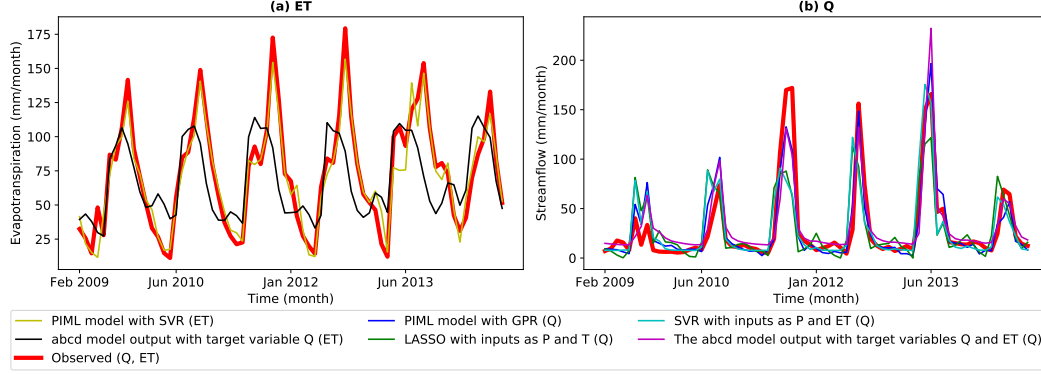


Figure 7. Time series plots of observed streamflow and evapotranspiration with modeled outputs of the best of all the models (the abcd model, ML models and PIML models): (a) evapotranspiration (ET) and (b) streamflow (Q).

Table 5. Annual water balance analysis of physics-informed data science model for testing period (2009-2014). All the values are in mm.

Model/observed	P	ET	Q	ET + Q	Percentage of deviation
Observed	1231.783	878.549	363.118	1241.667	0
PIML with SVR	1231.783	856.204	345.053	1201.257	-3.255
PIML with GPR	1231.783	796.954	360.847	1157.801	-6.754
PIML with SVR and GPR	1231.783	856.204	361.962	1218.166	-1.893

The proposed PIML model is the first-of-its-kind to provide an intuitive way to combine physically interpretable architectures of lumped hydrological models with state-of-the-art ML algorithms in a meaningful way. We also study the ability of these models to quantify uncertainties in both intermediate and target variables. For our study area, outputs from the PIML model exhibited high prediction performance compared to pure physics-based or ML approaches. Besides, we observe a significant reduction in the uncertainty bounds for predictions of both variables. We also assessed the ability of the PIML models to simulate the annual water budget and noted consistent performance for various variants.

The PIML model presented in this manuscript allows us to capture complex and non-linear dependencies between hydrological variables while being mindful of the logical sequence which the physics-based model guides. The proposed approach provides a way to add flexibility to otherwise rigid model structures of state-of-the-art hydrological models widely used in hydrology. While we demonstrate the applicability of this approach using a simple WB model (*abcd* model), this approach can be extended to other conceptual models, which may involve a much larger number of intermediate steps.

Future extensions to the PIML framework for hydrological applications need to be validated for distributed as well as semi-distributed model structures, as well as for daily and sub-daily time-steps. Moreover, we have ignored the role of upstream reservoirs, which might impact the predictive skills of models, especially at daily and sub-daily scales. Also,

the performance of the PIML model is highly sensitive to the choice of ML algorithms used at various intermediate steps. As of now, there are no proven guidelines on the best ML model selection. Despite these outlined limitations, the application of the proposed framework can be extended to various scientific and engineering problems such as early warning systems, risk and reliability assessment for hydraulic structures, and flood management.

Acknowledgments

Funding for the project is provided by Scheme for Transformational and Advances in Sciences of Ministry of Education implemented by Indian Institute of Science, Bangalore (Research Project ID: 367 titled 'Physics Guided Data Science Approach for Predictive Understanding of Hydrological Processes'). The authors thank Professor Auroop Ganguly from Northeastern University, Boston for helpful discussions, and IIT Gandhinagar colleagues Professor Nipun Batra, and Divya Upadhyay for comments on the manuscript.

References

- Alley, W. M. (1984). On the treatment of evapotranspiration, soil moisture accounting, and aquifer recharge in monthly water balance models. *Water Resources Research*, 20(8), 1137–1149.
- Bai, P., Liu, X., Liang, K., & Liu, C. (2015). Comparison of performance of twelve monthly water balance models in different climatic catchments of china. *Journal of Hydrology*, 529, 1030–1040.
- Beven, K. (1989). Changing ideas in hydrology—the case of physically-based models. *Journal of hydrology*, 105(1-2), 157–172.
- Beven, K. (2006). A manifesto for the equifinality thesis. *Journal of hydrology*, 320(1-2), 18–36.
- Blundell, C., Cornebise, J., Kavukcuoglu, K., & Wierstra, D. (2015, 07–09 Jul). Weight uncertainty in neural network. In F. Bach & D. Blei (Eds.), *Proceedings of the 32nd international conference on machine learning* (Vol. 37, pp. 1613–1622). Lille, France: PMLR. Retrieved from <http://proceedings.mlr.press/v37/blundell115.html>
- Butts, M. B., Payne, J. T., Kristensen, M., & Madsen, H. (2004). An evaluation of the impact of model structure on hydrological modelling uncertainty for streamflow simulation. *Journal of hydrology*, 298(1-4), 242–266.
- Cheng, M., Fang, F., Kinouchi, T., Navon, I., & Pain, C. (2020). Long lead-time daily and monthly streamflow forecasting using machine learning methods. *Journal of Hydrology*, 590, 125376.
- Chokmani, K., Ouarda, T. B., Hamilton, S., Ghedira, M. H., & Gingras, H. (2008). Comparison of ice-affected streamflow estimates computed using artificial neural networks and multiple regression techniques. *Journal of Hydrology*, 349(3-4), 383–396.
- Clark, M. P., & Kavetski, D. (2010). Ancient numerical demons of conceptual hydrological modeling: 1. fidelity and efficiency of time stepping schemes. *Water Resources Research*, 46(10).
- Deka, P. C., et al. (2014). Support vector machine applications in the field of hydrology: a review. *Applied soft computing*, 19, 372–386.
- Devia, G. K., Ganasri, B. P., & Dwarakish, G. S. (2015). A review on hydrological models. *Aquatic Procedia*, 4, 1001–1007.
- Dibike, Y. B., Velickov, S., Solomatine, D., & Abbott, M. B. (2001). Model induction with support vector machines: introduction and applications. *Journal of Computing in Civil Engineering*, 15(3), 208–216.
- Esposito, P. (2020). *Blitz - bayesian layers in torch zoo (a bayesian deep learning library for torch)*. <https://github.com/piEsposito/blitz-bayesian-deep>

-learning/. GitHub.

- Faghmous, J. H., Banerjee, A., Shekhar, S., Steinbach, M., Kumar, V., Ganguly, A. R., & Samatova, N. (2014). Theory-guided data science for climate change. *Computer*, 47(11), 74–78.
- Feng, D., Fang, K., & Shen, C. (2020). Enhancing streamflow forecast and extracting insights using long-short term memory networks with data integration at continental scales. *Water Resources Research*, 56(9), e2019WR026793.
- Fenicia, F., Savenije, H. H., Matgen, P., & Pfister, L. (2007). A comparison of alternative multiobjective calibration strategies for hydrological modeling. *Water Resources Research*, 43(3).
- Fu, M., Fan, T., Ding, Z., Salih, S. Q., Al-Ansari, N., & Yaseen, Z. M. (2020). Deep learning data-intelligence model based on adjusted forecasting window scale: application in daily streamflow simulation. *IEEE Access*, 8, 32632–32651.
- Ganguly, A. R., Kodra, E. A., Agrawal, A., Banerjee, A., Boriah, S., Chatterjee, S., ... Wuebbles, D. (2014). Toward enhanced understanding and projections of climate extremes using physics-guided data mining techniques. *Nonlinear Processes in Geophysics*, 21(4), 777–795. Retrieved from <https://npg.copernicus.org/articles/21/777/2014/> doi: 10.5194/npg-21-777-2014
- Gilpin, L. H., Bau, D., Yuan, B. Z., Bajwa, A., Specter, M., & Kagal, L. (2018). Explaining explanations: An overview of interpretability of machine learning. In *2018 IEEE 5th international conference on data science and advanced analytics (dsaa)* (pp. 80–89).
- Hargreaves, G. H., & Samani, Z. A. (1985). Reference crop evapotranspiration from temperature. *Applied engineering in agriculture*, 1(2), 96–99.
- Hochreiter, S., & Schmidhuber, J. (1997). Long short-term memory. *Neural computation*, 9(8), 1735–1780.
- Hoerl, A. E., & Kennard, R. W. (1970). Ridge regression: Biased estimation for nonorthogonal problems. *Technometrics*, 12(1), 55–67.
- Jia, X., Willard, J., Karpatne, A., Read, J., Zwart, J., Steinbach, M., & Kumar, V. (2019). Physics guided rnns for modeling dynamical systems: A case study in simulating lake temperature profiles. In *Proceedings of the 2019 siam international conference on data mining* (pp. 558–566).
- Karpatne, A., Watkins, W., Read, J., & Kumar, V. (2017). Physics-guided neural networks (pgnn): An application in lake temperature modeling. *arXiv preprint arXiv:1710.11431*.
- Khandelwal, A., Xu, S., Li, X., Jia, X., Steinbach, M., Duffy, C., ... Kumar, V. (2020). Physics guided machine learning methods for hydrology. *arXiv preprint arXiv:2012.02854*.
- Kirchner, J. W. (2006). Getting the right answers for the right reasons: Linking measurements, analyses, and models to advance the science of hydrology. *Water Resources Research*, 42(3).
- Kratzert, F., Klotz, D., Brenner, C., Schulz, K., & Herrnegger, M. (2018). Rainfall-runoff modelling using long short-term memory (lstm) networks. *Hydrology and Earth System Sciences*, 22(11), 6005–6022.
- Lange, H., & Sippel, S. (2020). Machine learning applications in hydrology. In *Forest-water interactions* (pp. 233–257). Springer.
- Li, B., Rodell, M., Sheffield, J., Wood, E., & Sutanudjaja, E. (2019). Long-term, non-anthropogenic groundwater storage changes simulated by three global-scale hydrological models. *Scientific reports*, 9(1), 1–13.
- Li, W., & Sankarasubramanian, A. (2012). Reducing hydrologic model uncertainty in monthly streamflow predictions using multimodel combination. *Water Resources Research*, 48(12).
- Liang, J., Li, W., Bradford, S. A., & Simunek, J. (2019). Physics-informed data-driven models to predict surface runoff water quantity and quality in agricul-

- tural fields. *Water*, 11(2), 200.
- Lima, C. H., & Lall, U. (2010). Climate informed monthly streamflow forecasts for the brazilian hydropower network using a periodic ridge regression model. *Journal of hydrology*, 380(3-4), 438–449.
- Lu, D., Konapala, G., Painter, S. L., Kao, S.-C., & Gangrade, S. (2021). Streamflow simulation in data-scarce basins using bayesian and physics-informed machine learning models. *Journal of Hydrometeorology*.
- Maity, R., Bhagwat, P. P., & Bhatnagar, A. (2010). Potential of support vector regression for prediction of monthly streamflow using endogenous property. *Hydrological Processes: An International Journal*, 24(7), 917–923.
- Malik, A., Tikhamarine, Y., Souag-Gamane, D., Kisi, O., & Pham, Q. B. (2020). Support vector regression optimized by meta-heuristic algorithms for daily streamflow prediction. *Stochastic Environmental Research and Risk Assessment*, 34(11), 1755–1773.
- Marshall, L., Nott, D., & Sharma, A. (2004). A comparative study of markov chain monte carlo methods for conceptual rainfall-runoff modeling. *Water Resources Research*, 40(2).
- Martinez, G. F., & Gupta, H. V. (2010). Toward improved identification of hydrological models: A diagnostic evaluation of the “abcd” monthly water balance model for the conterminous united states. *Water Resources Research*, 46(8).
- McCuen, R. H., Knight, Z., & Cutter, A. G. (2006). Evaluation of the nash–sutcliffe efficiency index. *Journal of hydrologic engineering*, 11(6), 597–602.
- Moriasi, D. N., Gitau, M. W., Pai, N., & Daggupati, P. (2015). Hydrologic and water quality models: Performance measures and evaluation criteria. *Transactions of the ASABE*, 58(6), 1763–1785.
- Muralidhar, N., Bu, J., Cao, Z., He, L., Ramakrishnan, N., Tafti, D., & Karpatne, A. (2019). Physics-guided design and learning of neural networks for predicting drag force on particle suspensions in moving fluids. *arXiv preprint arXiv:1911.04240*.
- Najafi, M. R., & Moradkhani, H. (2016). Ensemble combination of seasonal streamflow forecasts. *Journal of Hydrologic Engineering*, 21(1), 04015043.
- Nash, J. E., & Sutcliffe, J. V. (1970). River flow forecasting through conceptual models part i—a discussion of principles. *Journal of hydrology*, 10(3), 282–290.
- Neitsch, S., Arnold, J., Kiniry, J., Srinivasan, R., & Williams, J. (2004). Soil and water assessment tool input/output file documentation, version 2005: Temple, tx. *US Department of Agriculture, Agricultural Research Service, Grassland, Soil and Water Research Laboratory, available online at:” ftp://ftp.brc.tamus.edu/pub/outgoing/sammons/swat2005” (accessed 11/28/06)*.
- Niu, W.-j., & Feng, Z.-k. (2021). Evaluating the performances of several artificial intelligence methods in forecasting daily streamflow time series for sustainable water resources management. *Sustainable Cities and Society*, 64, 102562.
- Pai, D., Sridhar, L., Rajeevan, M., Sreejith, O., Satbhai, N., & Mukhopadhyay, B. (2014). Development of a new high spatial resolution (0.25×0.25) long period (1901–2010) daily gridded rainfall data set over india and its comparison with existing data sets over the region. *Mausam*, 65(1), 1–18.
- Parisouj, P., Mohebzadeh, H., & Lee, T. (2020). Employing machine learning algorithms for streamflow prediction: a case study of four river basins with different climatic zones in the united states. *Water Resources Management*, 34(13), 4113–4131.
- Paul, P. K., Gaur, S., Kumari, B., Panigrahy, N., Mishra, A., & Singh, R. (2019). Diagnosing credibility of a large-scale conceptual hydrological model in simulating streamflow. *Journal of Hydrologic Engineering*, 24(4), 04019004.
- Raje, D., & Krishnan, R. (2012). Bayesian parameter uncertainty modeling in a macroscale hydrologic model and its impact on indian river basin hydrology

- under climate change. *Water Resources Research*, 48(8).
- Rasouli, K., Hsieh, W. W., & Cannon, A. J. (2012). Daily streamflow forecasting by machine learning methods with weather and climate inputs. *Journal of Hydrology*, 414, 284–293.
- Reichstein, M., Camps-Valls, G., Stevens, B., Jung, M., Denzler, J., Carvalhais, N., & Prabhat. (2019). Deep learning and process understanding for data-driven earth system science. *Nature*, 566(7743), 195–204.
- Schmidt, L., Heße, F., Attinger, S., & Kumar, R. (2020). Challenges in applying machine learning models for hydrological inference: A case study for flooding events across germany. *Water Resources Research*, 56(5).
- Srivastava, A., Rajeevan, M., & Kshirsagar, S. (2009). Development of a high resolution daily gridded temperature data set (1969–2005) for the indian region. *Atmospheric Science Letters*, 10(4), 249–254.
- Sun, A. Y., Wang, D., & Xu, X. (2014). Monthly streamflow forecasting using gaussian process regression. *Journal of Hydrology*, 511, 72–81.
- Swain, J. B., & Patra, K. C. (2017). Streamflow estimation in ungauged catchments using regionalization techniques. *Journal of Hydrology*, 554, 420–433.
- Szilagyi, J. (2020). Water balance backward: Estimation of annual watershed precipitation and its long-term trend with the help of the calibration-free generalized complementary relationship of evaporation. *Water*, 12(6), 1775.
- Thomas, H. (1981). Improved methods for national water assessment. *Report WR15249270, US Water Resource Council, Washington, DC*.
- Tibshirani, R. (1996). Regression shrinkage and selection via the lasso. *Journal of the Royal Statistical Society: Series B (Methodological)*, 58(1), 267–288.
- Tongal, H., & Booij, M. J. (2018). Simulation and forecasting of streamflows using machine learning models coupled with base flow separation. *Journal of hydrology*, 564, 266–282.
- Vandewiele, G., Xu, C.-Y., et al. (1992). Methodology and comparative study of monthly water balance models in belgium, china and burma. *Journal of Hydrology*, 134(1-4), 315–347.
- Vapnik, V. N. (1995). *The nature of statistical learning theory*. Springer-Verlag.
- Vieux, B. E., Cui, Z., & Gaur, A. (2004). Evaluation of a physics-based distributed hydrologic model for flood forecasting. *Journal of hydrology*, 298(1-4), 155–177.
- Wagena, M. B., Goering, D., Collick, A. S., Bock, E., Fuka, D. R., Buda, A., & Easton, Z. M. (2020). Comparison of short-term streamflow forecasting using stochastic time series, neural networks, process-based, and bayesian models. *Environmental Modelling & Software*, 126, 104669.
- Wagner, N., & Rondinelli, J. M. (2016). Theory-guided machine learning in materials science. *Frontiers in Materials*, 3, 28.
- Wang, J.-X., Wu, J.-L., & Xiao, H. (2017). Physics-informed machine learning approach for reconstructing reynolds stress modeling discrepancies based on dns data. *Physical Review Fluids*, 2(3), 034603.
- Williams, C. K., & Rasmussen, C. E. (2006). *Gaussian processes for machine learning* (Vol. 2) (No. 3). MIT press Cambridge, MA.
- Xiang, Z., Yan, J., & Demir, I. (2020). A rainfall-runoff model with lstm-based sequence-to-sequence learning. *Water resources research*, 56(1), e2019WR025326.
- Xiong, M., Liu, P., Cheng, L., Deng, C., Gui, Z., Zhang, X., & Liu, Y. (2019). Identifying time-varying hydrological model parameters to improve simulation efficiency by the ensemble kalman filter: A joint assimilation of streamflow and actual evapotranspiration. *Journal of Hydrology*, 568, 758–768.
- Yang, J., Reichert, P., & Abbaspour, K. C. (2007). Bayesian uncertainty analysis in distributed hydrologic modeling: A case study in the thur river basin (switzerland). *Water resources research*, 43(10).

- Yang, T., Sun, F., Gentile, P., Liu, W., Wang, H., Yin, J., . . . Liu, C. (2019). Evaluation and machine learning improvement of global hydrological model-based flood simulations. *Environmental Research Letters*, *14*(11), 114027.
- Yu, X., & Liong, S.-Y. (2007). Forecasting of hydrologic time series with ridge regression in feature space. *Journal of Hydrology*, *332*(3-4), 290–302.
- Zhang, R., Liu, Y., & Sun, H. (2020). Physics-guided convolutional neural network (phycnn) for data-driven seismic response modeling. *Engineering Structures*, *215*, 110704.